



Contents lists available at ScienceDirect

# Journal of the Mechanical Behavior of Biomedical Materials

journal homepage: [www.elsevier.com/locate/jmbbm](http://www.elsevier.com/locate/jmbbm)

## Effects of different surface treatments on the cyclic fatigue strength of one-piece CAD/CAM zirconia implants

Qian Ding<sup>a</sup>, Lei Zhang<sup>a,\*</sup>, Rui Bao<sup>c</sup>, Gang Zheng<sup>b</sup>, Yuchun Sun<sup>d</sup>, Qiufei Xie<sup>a</sup><sup>a</sup> Department of Prosthodontics, Peking University School and Hospital of Stomatology, 22 South Street ZhongGuanCun, Haidian District, Beijing 100081, China<sup>b</sup> Department of Dental Materials, Peking University School and Hospital of Stomatology; National Engineering Laboratory for Digital and Material Technology of Stomatology, Peking University, 22 South Street ZhongGuanCun, Haidian District, Beijing 100081, China<sup>c</sup> Institute of Solid Mechanics, School of Aeronautic Science and Engineering, Beihang University, No. 37 Xueyuan Road, Haidian District, Beijing 100191, China<sup>d</sup> Center of Digital Dentistry, Peking University School and Hospital of Stomatology; National Engineering Laboratory for Digital and Material Technology of Stomatology; Research Center of Engineering and Technology for Digital Dentistry, Ministry of Health, 22 South Street ZhongGuanCun, Haidian District, Beijing 100081, China

## ARTICLE INFO

## Keywords:

Dental implant  
Zirconia  
CAD/CAM  
Fatigue  
Surface treatment

## ABSTRACT

**Objectives:** The effects of different surface treatments on cyclic fatigue strengths of computer-aided design and computer-aided manufacturing (CAD/CAM) zirconia implants and its mechanisms were evaluated.

**Material and methods:** One-piece cylindrical screw-type zirconia (Y-TZP) implants with diameters of 4.1-mm were fabricated using CAD/CAM technique; they were divided into four groups according to the type of surface treatment: (i) sintering (control group, CTRL), (ii) sandblasting (SB), (iii) sandblasting and etching with an experimental hot etching solution (SB-ST), and (iv) sandblasting and etching with hydrofluoric acid (SB-HF). The surface morphology and roughness of the implants were evaluated. Tetragonal to monoclinic transformation was measured on the surface by micro Raman spectroscopy. Static and fatigue tests were carried out at room temperature following the ISO 14801:2014 Standard. The cyclic fatigue strength of each group was determined using the staircase method. Specimens that survived the fatigue test were statically loaded to measure the residual fracture strength.

**Results:** Among the four groups, SB-HF exhibited the highest surface roughness. Compared with the CTRL group, the surface monoclinic content was higher after all three types of surface treatments, amongst which, SB-HF had the highest content (39.14%), significantly more than the other three groups ( $P < 0.01$ ). The cyclic fatigue strengths of CTRL, SB, SB-ST, and SB-HF implants were 530 N, 662.5 N, 705 N, and 555 N, respectively. The fracture strength after fatigue loading was higher than that before fatigue loading with no significant difference ( $P > 0.05$ ).

**Conclusions:** SB and SB-ST remarkably enhanced the fatigue resistance of zirconia implants, while SB-HF did not. One-piece 4.1-mm diameter CAD/CAM zirconia implants have sufficient durability for application in dental implants.

### 1. Introduction

In the recent years, yttria-stabilized tetragonal zirconia polycrystal (Y-TZP), a high-strength zirconia ceramic, has become an attractive new material for dental implants. Zirconia has tooth-like color and the ability to transmit light, improving the overall esthetic outcome (Oliva et al., 2010). Moreover, it has a high chemical resistance, high flexural strength (900–1200 MPa), a favorable fracture toughness ( $K_{IC}$ , 7–10 MPa m<sup>1/2</sup>), and a suitable Young's modulus (210 GPa) (Ozkurt and Kazazoglu, 2011). Another advantage is the less affinity for dental plaque, minimizing the risk of inflammatory changes in the surrounding

soft tissues (Scarano et al., 2010; Tete et al., 2009).

Both the implant body and the perimucosal portion can be individually designed to fit the local anatomical conditions and digitally machined. One-piece implants have the advantage of no implant/abutment movement or gap causing the leakage of harmful bacteria, as observed with conventional implant/abutment connections (Assenza et al., 2012). Because of the abovementioned advantages, Y-TZP implants have the potential to be an effective alternative of titanium implants in certain clinical situations (Andriotelli et al., 2009; Oliva et al., 2010) as well as an appropriate material for computer-aided design and computer-aided manufacturing (CAD/CAM).

Abbreviations: CTRL, control group; SB, sandblasting group; SB-ST, sandblasting and acid etching group; SB-HF, sandblasting and 40% hydrofluoric acid etching group

\* Corresponding author.

E-mail address: [drzhanglei@yeah.net](mailto:drzhanglei@yeah.net) (L. Zhang).

<https://doi.org/10.1016/j.jmbbm.2018.05.002>

Received 8 March 2018; Received in revised form 26 April 2018; Accepted 2 May 2018

Available online 03 May 2018

1751-6161/ © 2018 Elsevier Ltd. All rights reserved.

Previous clinical studies have reported promising survival rates of 98%, 96.5%, and 95% at 1, 3, and 5 years, respectively, after the placement of zirconia implants with rough surface topographies in partially edentulous patients (Brull et al., 2014; Oliva et al., 2010, 2007). However, one study also reported a low survival rate of 77.3% after a mean follow-up period of 5.94 years. Furthermore, 18 implants failed because of fracture, mostly occurring in narrow implants with 3.25 mm in diameter (15/18) (Roehling et al., 2015).

The fracture of a dental implant is always a severe complication, leading to a high level of patient discomfort and many clinical problems such as the difficulty in removing the fractured implant and significant bone loss (Gahlert et al., 2012). Implant fractures in clinical use were caused by fatigue under physiological loads, and those failures were aggravated by the resorption of bone around the implants (Gahlert et al., 2012; Morgan et al., 1993). Static loading may have very slight clinical relevance as mechanical failures are more probably related to the application of repeated loads rather than an acute overload (Lee et al., 2009). As an important part of the mechanical properties of zirconia implants, fatigue is considered to be one of the key factors affecting the long-term clinical effect of the implants and their restoration (Rita Depprich, 2012).

Pure zirconium dioxide has three crystallographic forms that are stable at different temperature ranges under atmospheric pressure: the monoclinic phase, which is stable up to 1170 °C, where it transforms to the tetragonal phase, which in turn is stable up to 2370 °C, and the cubic phase, which exists up to its melting point of 2680 °C (Denry and Kelly, 2008). However, the tetragonal phase is in fact “metastable” at room temperature and may transform into the monoclinic phase, which can be triggered by mechanical stress, thermal aging, chemical aging, and intermittent forces during mastication in the oral environment (Guazzato et al., 2004; Pittayachawan et al., 2009).

Previous studies have demonstrated that surface modifications enhanced the integration of zirconia implants and resulted in a better osseointegration compared to the unmodified surface (Gahlert et al., 2007; Sennerby et al., 2005). Surface modifications such as sandblasting and acid etching trigger tetragonal-to-monoclinic ( $t \rightarrow m$ ) phase transformation (Karakoca and Yilmaz, 2009). This transformation is associated with 3–4% phase volume expansion and induces compressive stresses that shield the crack tip from the applied stress (Porter and Heuer, 1977). This unique characteristic is known as transformation toughening and may explain the increased fracture strength and fracture toughness of Y-TZP ceramics compared to other dental ceramics (Piconi and Maccauro, 1999).

On the other hand, the surface flaws introduced by sandblasting and acid etching act as stress concentrators and may become potential sites for crack initiation and propagation, causing strength degradation (Wang et al., 2008). The macroscopic and microscopic failure analysis in a clinical research showed that the presence of microcracks on a surface due to the manufacturing process, including machining and surface treatments, may be one of the primary reasons for zirconia implant fracture (Gahlert et al., 2012).

However, studies focused on the fatigue of zirconia implants after different surface treatments and the related mechanism are rare and are urgently required prior to consideration for routine clinical applications. Therefore, the aim of this study was to evaluate the effects of four different surface treatments on the cyclic fatigue strength and phase transformation of CAD/CAM Y-TZP implants.

## 2. Material and methods

### 2.1. Fabrication of zirconia implants

One-piece cylindrical screw-type zirconia implants were designed using the three-dimensional (3D) CAD software (Catia V5R19, Dassault System, France; Geomagic Studio 12.0, Geomagic, USA) and fabricated using the following procedure. To reduce processing time and wear of



Fig. 1. CAD/CAM one-piece Y-TZP implants with diameters of 4.1 mm.

the cutting instruments during the milling process, partially sintered Y-TZP blocks instead of fully sintered ones were used in this study. First, partially sintered zirconia milling blocks (Y-TZP, Wieland, Germany) were cut using a diamond wheel in a cutting machine (Zenotec Mini, Wieland, Germany) based on the CAM technology (Wieland CAM 2.2, Germany), followed by final sintering in a sintering furnace (Zeno Fire P1, Wieland, Germany). All the implants had an intraosseous length of 12 mm, diameters of 4.1 mm, and spiral threads with a 1.2-mm pitch and 0.25-mm depth (Fig. 1).

### 2.2. Surface treatment of implants

CAD/CAM one-piece zirconia implants with diameters of 4.1 mm were divided into four groups according to different surface treatments as follows:

- (1) Sintering group (CTRL), implants with a sintered surface.
- (2) Sandblasting group (SB), implants with a sandblasted surface. Sandblasting was performed using 110- $\mu\text{m}$   $\text{Al}_2\text{O}_3$  particles from a distance of 10–20 mm and at an angle of 90°. The air pressure used for the blasting was set at 0.45 MPa (Ovaljet HiBlaster, SHOFU, Japan).
- (3) Sandblasting and experimental hot etching group (SB-ST),

including implants with a sandblasted and acid-etched surface etched with an experimental hot etching solution. The experimental hot etching solution (100 mL) was composed of 80 mL methanol, 20 mL 37% hydrochloric acid (HCl), and 0.2 g ferric chloride. This solution was heated to 100 °C and applied for 60 min following a protocol reported by Casucci (Casucci et al., 2009) to improve the bonding potential of zirconia ceramics.

- (4) Sandblasting and hydrofluoric acid etching group (SB-HF), comprised of implants with a sandblasted and hydrofluoric acid-etched surface. After sandblasting, specimens were immersed in 40% hydrofluoric acid for 1 h at ambient temperature (Flamant and Anglada, 2016).

To avoid the interference of surface impurities on the surface measurements. All the implants were sequentially washed with absolute alcohol and deionized water (dH<sub>2</sub>O; Milli-Q Ultra-Pure, Millipore, Billerica, MA) in an ultrasonic cleaner for 15 min each. Subsequently, the specimens were dried at room temperature for 24 h. The surface topography of the implants was qualitatively analyzed using a scanning electron microscope (SEM; JEOL, JSM-6010LA, Tokyo, Japan) and quantitatively measured using a 3D laser scanning equipment (3D Laser Microscope VK-9700K, Keyence Co., Osaka, Japan). The following parameters were used to characterize the surface topography: Ra value, the arithmetic mean deviation of a profile; Rq value, the root-mean-square deviation of the profile; and Rz value, the 10-point height, i.e., the average height of the five lowest valleys and five highest peaks within the profile.

### 2.3. Micro Raman spectroscopy

Phase transformation (t-m) on the surface of the endosseous part of the zirconia implants was detected by micro Raman spectroscopy equipped with a triple monochromator spectrometer (LabRAM HR800, Horiba Jobin Yvon, France) and a CCD detector (liquid nitrogen cooled). A laser (argon ion, green monochromatic light) of 532 nm wavelength and 20 mW power at sample was used as the light source and three measurements per implant were carried out at the relatively flat part between the threads. Raman spectra were collected at 100× magnification and the spectrum integration time was 60 s. The spectra were analyzed using a double monochromator with a focal length of 0.8 mm and equipped with a diffraction grating with 1800 grooves/mm. The beam diameter was 1 μm with a spectral resolution of about 2 cm<sup>-1</sup>. The peaks related to the monoclinic phase appeared at 180 and 190 cm<sup>-1</sup>. The fraction of monoclinic phase can be calculated according to the equation given by Katagiri et al. (Katagiri et al., 1988):

$$V_m = 0.5 * (I_{m(180)} + I_{m(190)}) / [2.2 * I_{t(150)} + 0.5 * (I_{m(180)} + I_{m(190)})]$$

where  $I_{m(180)}$  and  $I_{m(190)}$  represent the intensities of the characteristic monoclinic peaks and  $I_{t(148)}$  represents the intensity of the tetragonal peak.

### 2.4. Mechanical testing

The mechanical tests were carried out following the ISO 14801:2014 Standard (2014). The zirconia implants were embedded in an acrylic resin (Denture base polymer I-type, NISSIN, Japan), 3 mm apically from the nominal bone level, simulating 3 mm of the marginal bone loss, and placed in an angle of 30° with respect to the vertical axis of the implant (Fig. 2). The test was conducted at room temperature. The loading force (F) of the testing machine was applied through the hemispherical chamber of a cobalt-chromium alloy crown with a radius of 3 mm and a distance of 11 ± 0.5 mm between the simulated bone level and the center of the hemisphere, which was adhered to the connecting part of each implant for load transfer. The steel jig was individually fabricated using an angle adjustable stand. The overall setup for the mechanical tests is shown in Fig. 2.

#### 2.4.1. Static testing

First, the test was carried out statically to determine the 30° flexural resistance of the implants. Three specimens from each group were used to measure the load-deflection curve using a universal testing machine (5900, Instron, USA) controlled using the Blue Hill testing software (Bluehill2, Instron, USA). A perpendicular load was applied to the angulated specimens under a crosshead speed of 1 mm/min. Fracture strength (N) was measured at the load at which the fracture occurred. T-tests were performed to determine the statistically significant differences between the four groups. A P-value of < 0.05 was considered statistically significant.

#### 2.4.2. Fatigue testing

A fatigue testing machine (ElectroPuls 1000, Instron, USA) with 1000 N-load capacity controlled by the Console and WaveMatrix™ dynamic testing software (Instron, USA) was used to perform the fatigue tests. The tests were carried out with a unidirectional cyclic load varying sinusoidally between a nominal peak value and 10% of this value for 5 × 10<sup>6</sup> cycles or until the failure. The frequency was 15 Hz. The maximum of 5 × 10<sup>6</sup> testing cycles set in this study has been widely reported to be approximately 25 years of intraoral usage (Huang et al., 2005). Therefore, in the fatigue analysis, the tests were considered to have been successfully completed if the implant survived up to 5 × 10<sup>6</sup> loading cycles.

The cyclic fatigue limit load in each group was determined by the staircase method (up-and-down method). Stress was raised in increments of < 5% of the estimated fatigue limit load, which was determined to be approximately 60% of the fracture strength in the static test of the same group. First, the estimated fatigue limit load was applied to a specimen. If the specimen fractured, the load was reduced by one increment in the next specimen. If the specimen survived, a load one increment higher was applied to the next specimen. This procedure was repeated until at least four couples of specimens with opposite results (fractures or survive) were observed, and the up-and-down chart was closed. The arithmetic mean value ( $m$ ) and standard deviation ( $\sigma$ ) of the fatigue limit load were determined by the staircase method. The calculation was carried out using the following equations (2014).

$$m = \sum_{i=1}^n (f_i + 0.5d) / n$$

$$\sigma = \sum_{i=1}^n (f_i - m)^2 / (n-1)$$

where  $f_i$  is the load used for the testing of a specimen,  $n$  is the total number of specimens used in the calculation, and  $d$  is the load increment. The fatigue limit load can then be expressed as follows:  $m \pm \sigma$ .

The fatigue fracture surfaces of the failed dental implants were gold-sputtered and investigated using a SEM (JSM-6010LA, JEOL, Tokyo, Japan). The SEM photographs were recorded at 40× and 1000× magnifications for image analysis. Using the SEM, the origin of the crack was identified, and images were obtained along the path of crack propagation.

#### 2.4.3. Static testing after fatigue loading

Specimens that survived the fatigue loading were loaded until fracture using the universal testing machine in exactly the same manner as the static testing. T-tests were performed to determine the statistically significant differences between the four groups and between fracture strength before and after fatigue loading. A P-value of < 0.05 was considered statistically significant.

## 3. Results

### 3.1. Microscopic observation and surface roughness of implants

The SEM images show that the CTRL surface is relatively flat with flaws such as notches and dents due to the CAM process (Luthardt et al.,

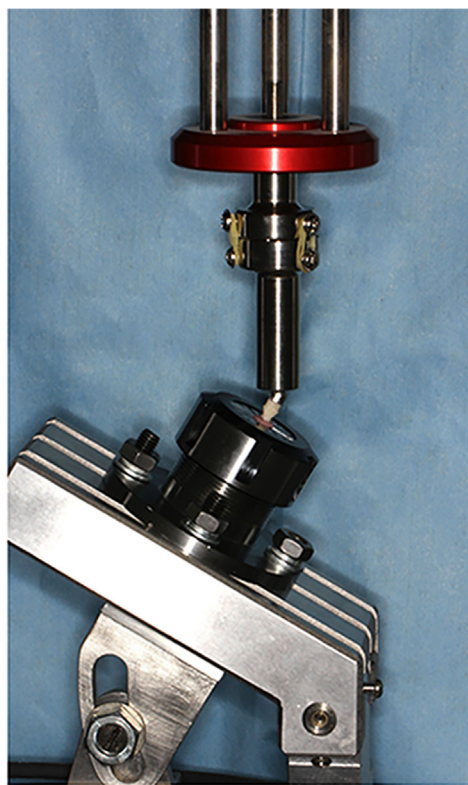
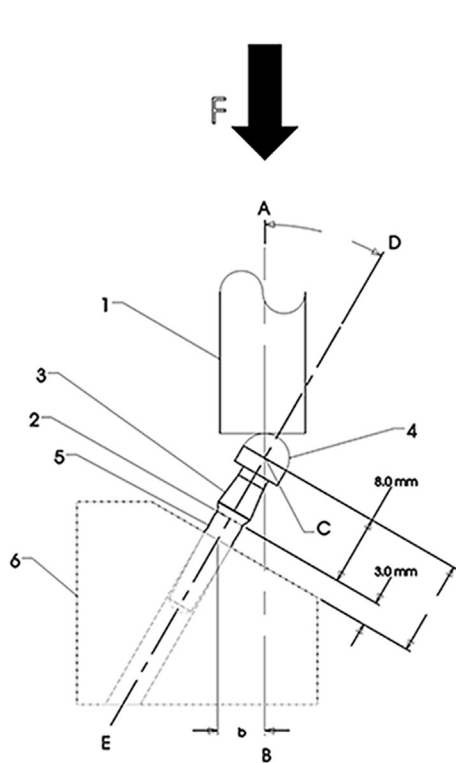


Fig. 2. Schematic and image of the testing machine and test set-up for cyclic fatigue test. 1, loading device; 2, nominal bone level; 3, abutment; 4, hemispherical loading member; 5, dental implant body; 6, specimen holder; F, the loading force. Point C, the loading center, intersection of the loading axis (Line AB) with the axis of the implant (Line DE), is well-defined.

2004). The surface of SB exhibited a macrorough topography with grooves and holes with sharp margins. After acid etching with experimental hot etching solution, the surfaces appeared uneven with peaks and valleys evident and nanoscale irregular pores. In contrast, the hydrofluoric acid etched surfaces exhibited a more regular porous topography in both the micrometer- and nanometric scale. (Fig. 3). The surface roughness levels are reported in Table 1. The Ra value significantly increased in the order CTRL < SB < SB-ST < SB-HF groups ( $P < 0.01$ ).

### 3.2. Phase transformation

Strong monoclinic bands appeared at Raman displacements of 180 and 190  $\text{cm}^{-1}$ , especially for the SB-HF surfaces (Fig. 4). Phase transformation analysis reveal that the monoclinic volume fraction increased slightly from  $15.68 \pm 1.07\%$  in the CTRL to  $16.89 \pm 0.86\%$  after sandblasting. Acid etching with experimental hot etching solution resulted in a significant monoclinic content increase to  $20.55 \pm 1.87\%$  ( $P < 0.05$ ). However, the highest estimated monoclinic volume fraction was calculated to be  $39.14 \pm 4.98\%$  for the SB-HF surfaces, significantly different to the other three groups ( $P < 0.01$ ).

### 3.3. Fracture strength in static testing (static strength)

Table 2 shows the average fracture strengths recorded for the four groups under static loading prior to fatigue loading. The fracture strength was higher in the SB and SB-ST groups than the CTRL group. The SB-ST samples exhibited the highest fracture strength, statistically similar to the SB samples and significantly different than the CTRL and SB-HF analogues ( $P < 0.01$ ). The average fracture strength of the SB-HF samples was statistically similar to the CTRL samples.

### 3.4. Cyclic fatigue limit load in fatigue testing (cyclic fatigue strength)

The results of fatigue limit in the cyclic fatigue tests were determined using the staircase method as shown in Fig. 5. The cyclic

fatigue strengths in the CTRL, SB, SB-ST, and SB-HF samples were 530 N, 662.5 N, 705 N, and 555 N, respectively (Table 2). The cyclic fatigue strength increased by 25% after sandblasting and by 33% after sandblasting and etching with the experimental hot acid solution, respectively. However, after hydrofluoric acid etching, the cyclic fatigue strength decreased by 20% on the basis of the SB samples, similar to the CTRL samples.

### 3.5. Fractographic analysis

Fig. 6 shows the SEM photographs of the fractured surfaces of specimens from six groups after the cyclic fatigue test. Most of the analyzed specimens exhibited processing flaws associated with fabrication and sintering; those flaws acted as stress concentrators during the crack nucleation. The fractured surface on the specimens of SB, SB-ST and SB-HF showed hackle lines radiating from the crack origin at the defect (red arrow) located on the surface or beneath the surface in the tensile stress side. A few inherent flaws such as pores and subsurface sintering dry spray agglomerate flaws were observed at the crack origins. However, on the sintered specimens, the crack origin was located at the tensile stress side surface between two threads. No obvious defects were observed on the crack origins of the CTRL samples.

### 3.6. Fracture strength after fatigue loading

The fracture strength averages after fatigue loading in the four groups are detailed in Table 2. Except for the SB group, fracture strength after fatigue loading increased compared to that before fatigue loading, especially in the CTRL group, which increased by 32.9%. The SB-ST group demonstrated the highest fracture strength after fatigue loading. No statistical difference was found between the four groups or between fracture strength before and after fatigue loading, in part due to fewer specimens being used in the static testing.

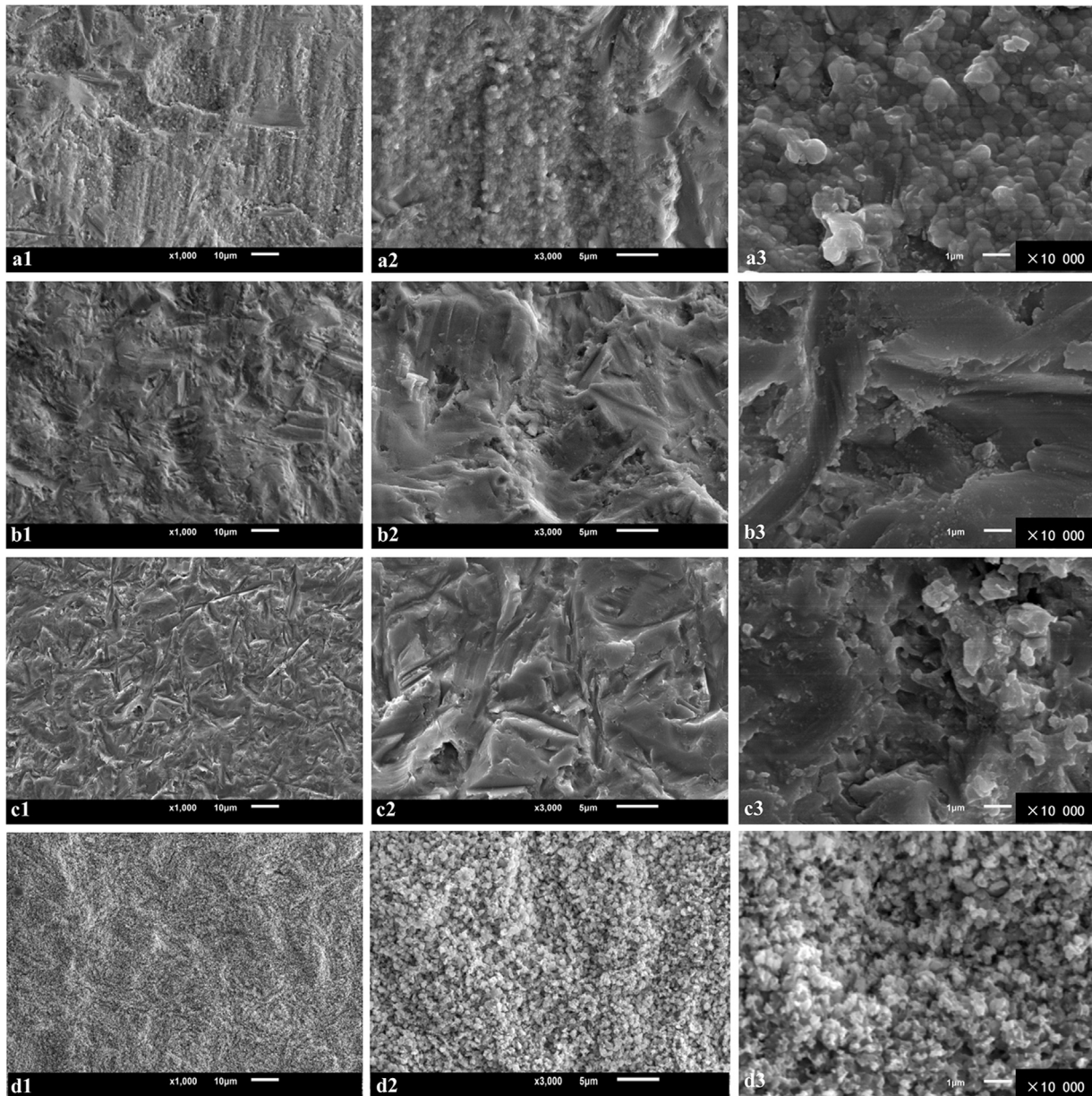


**Fig. 3.** SEM images showing the surface topographies of CAD/CAM zirconia implants in CTRL (a1–a3), SB (b1–b3), SB-ST (c1–c3), and SB-HF (d1–d3). CTRL, control group; SB, sandblasting group; SB-ST, sandblasting and acid etching with experimental hot etching solution; SB-HF, sandblasting and 40% hydrofluoric acid etching.

**Table 1**

Surface roughness of CAD/CAM zirconia implants ( $n = 3$ ). CTRL, control group; SB, sandblasting group; SB-ST, sandblasting and acid etching group; SB-HF, sandblasting and 40% hydrofluoric acid etching group. Values with different superscript letters are significantly different ( $P < 0.05$ ).

| Surface roughness ( $\mu\text{m}$ ) | Ra                | Rq                | Rz                 |
|-------------------------------------|-------------------|-------------------|--------------------|
| CTRL                                | 0.69 <sup>a</sup> | 0.89 <sup>a</sup> | 6.79 <sup>a</sup>  |
| SB                                  | 1.30 <sup>b</sup> | 1.69 <sup>b</sup> | 10.30 <sup>b</sup> |
| SB-ST                               | 1.49 <sup>c</sup> | 1.83 <sup>c</sup> | 12.92 <sup>c</sup> |
| SB-HF                               | 1.75 <sup>d</sup> | 2.14 <sup>d</sup> | 13.30 <sup>c</sup> |

## 4. Discussion

### 4.1. Effect of sandblasting or sandblasting and acid etching on the fatigue strength of zirconia implants

In this study, sandblasting with 110- $\mu\text{m}$   $\text{Al}_2\text{O}_3$  particles or

sandblasting and acid etching with an experimental hot solution improved the fatigue and fracture resistance of the CAD/CAM zirconia implants, which can be attributed to the transformation toughening of Y-TZP. The sandblasting and acid etching triggered  $t \rightarrow m$  phase transformation that induced compressive stresses, thus closing the crack tip and preventing further crack propagation (Ozcan et al., 2013; Porter and Heuer, 1977). The compressive effect of the residual stresses on the surface also hindered the crack nucleation (Gil et al., 2014). This fact can be observed in Fig. 5, where the crack initiates from the surface for the sintered specimen and from the subsurface for the sandblasted specimen.

Most previous studies (Chintapalli et al., 2014; Garcia et al., 2013; Kosma et al., 2008) have demonstrated that airborne particle abraded with 110- $\mu\text{m}$  or 120- $\mu\text{m}$   $\text{Al}_2\text{O}_3$  particles significantly increased the flexural strength of Y-TZP specimens, because of the transformation toughening mechanism that generated a compressive stress that opposed the externally applied, crack-propagating tensile stress of the specimen. A previous study (Gil et al., 2014) on titanium implants also

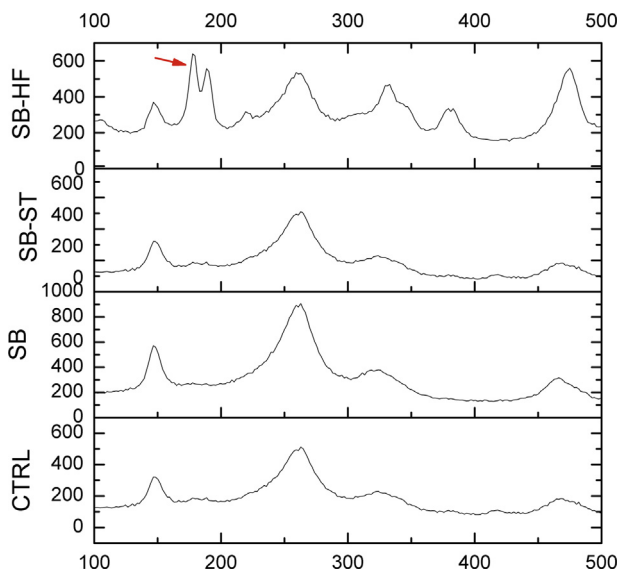


Fig. 4. Raman spectra of CAD/CAM zirconia implants. Red arrows indicate the strong monoclinic bands appearing at Raman displacements of 180 and 190  $\text{cm}^{-1}$  in the SB-HF group.

Table 2

Fracture and cyclic fatigue strengths of the four groups (mean  $\pm$  SD). CTRL, control group; SB, sandblasting group; SB-ST, sandblasting and acid etching with experimental hot etching solution; SB-HF, sandblasting and 40% hydrofluoric acid etching.

| Groups | Fracture strength before fatigue loading (N) | Cyclic fatigue strength (N) | Fracture strength after fatigue loading (N) |
|--------|--|-----------------------------|---|
| CTRL   | 827.3 $\pm$ 101.6                            | 530.0 $\pm$ 21.6            | 1099.3 $\pm$ 196.0                          |
| SB     | 1162.9 $\pm$ 116.5                           | 662.5 $\pm$ 21.2            | 1064.5 $\pm$ 209.2                          |
| SB-ST  | 1118.1 $\pm$ 166.6                           | 705.0 $\pm$ 20.7            | 1147.3 $\pm$ 69.9                           |
| SB-HF  | 867.2 $\pm$ 171.0                            | 555.0 $\pm$ 14.1            | 912.7 $\pm$ 100.4                           |

showed that the grit blasting of implants improved the fatigue life because of the formation of a layer of compressive residual stresses. Iijima (Iijima et al., 2013) reported that sandblasting decreased the flexural strength of Y-TZP. Moreover, a further decrease in the flexural strength was observed in sandblasted and acid-etched Y-TZP under both the static loading and cyclic fatigue tests. The conflicting results may be the consequence of different zirconia materials or techniques used in the surface treatments. Kosmac et al. (2000) reported that the phase transformation of Y-TZP strongly depends on the grain size.

In this study, micro Raman spectroscopy analysis showed that acid etching using both the experimental hot solution and hydrofluoric acid increased the  $t \rightarrow m$  transformation of zirconia. The former led to an increase in static and fatigue strengths of the implants, while the latter resulted in an opposite trend. Egilmez et al. (2014) reported that flexural strength significantly decreased after chemical degradation (acid etching) and increased through abrasion of airborne 110- $\mu\text{m}$   $\text{Al}_2\text{O}_3$  particles at 4 bar pressure compared to a sintered surface. Flamant and Anglada (2016) reported that 40% HF etching induced an increase in monoclinic phase content and a decrease in flexural strength limited to 15% for etching times below 60 min. Xie et al. (2015) reported that the flexural strength of Y-TZP was significantly deteriorated by chemical degradation with 40% HF at ambient temperature for 2 h. However, the flexural strength did not decrease when immersed in 5% HF for 1 and 5 days compared to the control group. This indicates that the degree of phase transformation or potential damage caused by acid etching played an important role in the variation in mechanical properties.

Some authors suggested that strength variation with phase transformation depends on a balance between the accumulation of

compressive stresses and microcracking occurring in the transformed areas (Sanon et al., 2013). Considering the positive and negative effects of sandblasting and acid-etching, it was believed that along with the progress of  $t \rightarrow m$  phase transformation during the surface treatment, the flexural and fatigue strengths would increase at the beginning. Therefore, an improvement in the fatigue behavior of SB and SB-ST was achieved. However, if the  $t \rightarrow m$  phase transformation occurs as a widespread surface feature, compressive stresses induced by the volume extension of transformed grains may result in microcrack formation and propagation, deteriorating the strength (Egilmez et al., 2014). In this study, the monoclinic volume fraction in the surfaces of the SB-HF samples was comparatively the highest, 39.14%, amongst the groups tested, while SB and SB-ST sample surfaces were only 16.89% and 20.55%, respectively. The results indicate that the degree of  $t \rightarrow m$  phase transformation in the SB-HF group resulted in more microcrack formation than in the SB and SB-ST groups, which may act to decrease strength.

There was already monoclinic phase in CTRL in this study. The reasons can be explained as follows. CAD/CAM machining of pre-sintered Y-TZP blocks induced compressive stresses and microcracks from the  $t \rightarrow m$  phase transformation. Then final sintering partially healed microcracks and eliminated flaws. It also facilitated the  $m \rightarrow t$  phase transformation and relieved surface compressive stresses (Kim et al., 2010; Raigrodski, 2004). But the SEM observations demonstrated that the surface microcracks and flaws were not fully healed by the final-sintering process and monoclinic phase still exist. Besides, ultrasonic cleaning in deionized water may also induced  $t \rightarrow m$  phase transformation on the surfaces of the zirconia implants (Sanon et al., 2013).

#### 4.2. Effect of fatigue loading on the static strength of zirconia implants

In this study, fracture strength after fatigue loading was higher than that before fatigue loading in three groups, especially in CTRL. One possible reason for this inconsistency is that specimens that survived fatigue loading may have less flaws and microcracks on the surface. Nemli et al. (2012) reported that fatigue with mechanical cycling over 20,000 cycles caused  $t \rightarrow m$  phase transformation on the surfaces of Y-TZP specimens, resulting in a significant increase in the fracture toughness. Thus, fatigue loading may also be an inducing factor for  $t \rightarrow m$  phase transformation. As described above, phase transformation within a certain limit could result in a fracture strength increase due to transformation toughening. The CTRL group contained the lowest monoclinic volume fraction before fatigue loading amongst the groups. This may explain the large increase in the fracture strength after fatigue loading in the CTRL group, which was speculated to benefit most from transformation toughening.

#### 4.3. Use of staircase method included in ISO14801:2014

The staircase method was used to estimate the fatigue strength in this study. Several testing methods have been developed for the mechanical evaluation of zirconia specimen or implants, such as the standard method using the S-N curve (ISO 14801) (Sevilla et al., 2010), single load-to-fracture (Sanon et al., 2015), fatigue followed by the application of a static load until fracture (Kohal et al., 2011), staircase method (ISO 14801) (Koyama et al., 2012), and step-stress accelerated life testing (Silva et al., 2009). Among these methods, the staircase method, which is included in ISO14801:2014 as an alternative to the S-N curve (ISO/DIS 14801 2014), automatically concentrates the testing near the mean and requires fewer tests. It is equally valid for determining the fatigue limit. ISO 14801 is an international normative standard that describes how to perform dynamic fatigue testing for single post, endosseous, transmucosal dental implants and simulates the functional loading of an endosseous implant body and its prosthetic components under the worst possible in vivo conditions. It was established for the evaluation of fracture and fatigue strength in implants

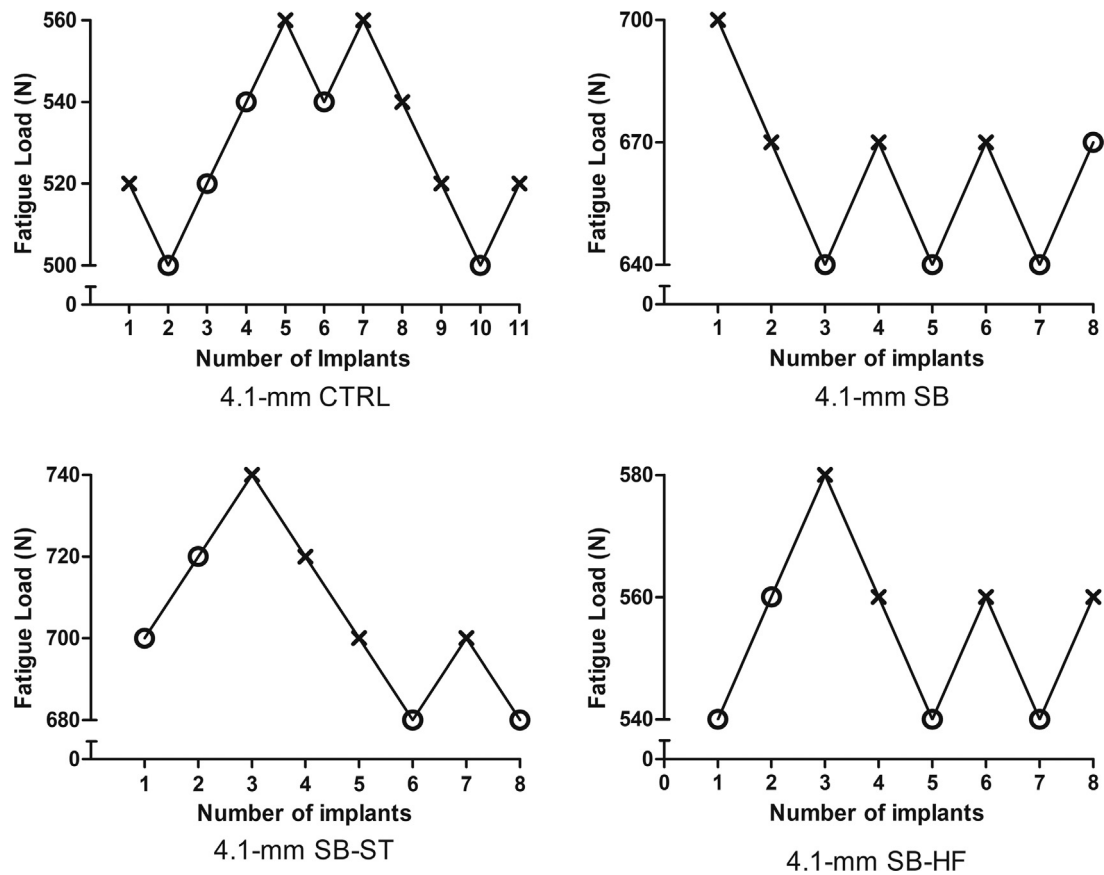


Fig. 5. Results of the staircase method: mean fatigue strength at  $5 \times 10^6$  cycles. × : Fracture, ○ : nonfracture.

and is recommended to be most useful for comparing endosseous dental implants of different designs.

#### 4.4. Fatigue performance of CAD/CAM zirconia implants

Sevilla et al. (2010) reported a similar fatigue limit ( $\sim 300$  N) for one-piece zirconia (4 mm) implants and two-piece titanium (3.8 mm) implants by mechanical testing following the ISO 14801 protocol. Another study (Gil et al., 2014) also reported a fatigue limit ranging from 315 N to 350 N for 3.8–4.2 mm titanium implants with different surface

treatments. Shemtov-Yona et al. (2014) investigated the fatigue performance of 5-mm titanium implants using an S-N curve; their fatigue limit load was 620 N. The degree of fatigue strength obtained in this study was superior to those of titanium and zirconia implants with a similar diameter reported in previous studies. Both the types of connection as well as the materials of the implant/abutment combination affect a system's resistance to failure. The failures of two-piece implant/abutment systems often involve the connecting screw. One-piece zirconia implants exhibited a higher fracture strength and reliability during the cyclic mechanical loading than two-piece zirconia and

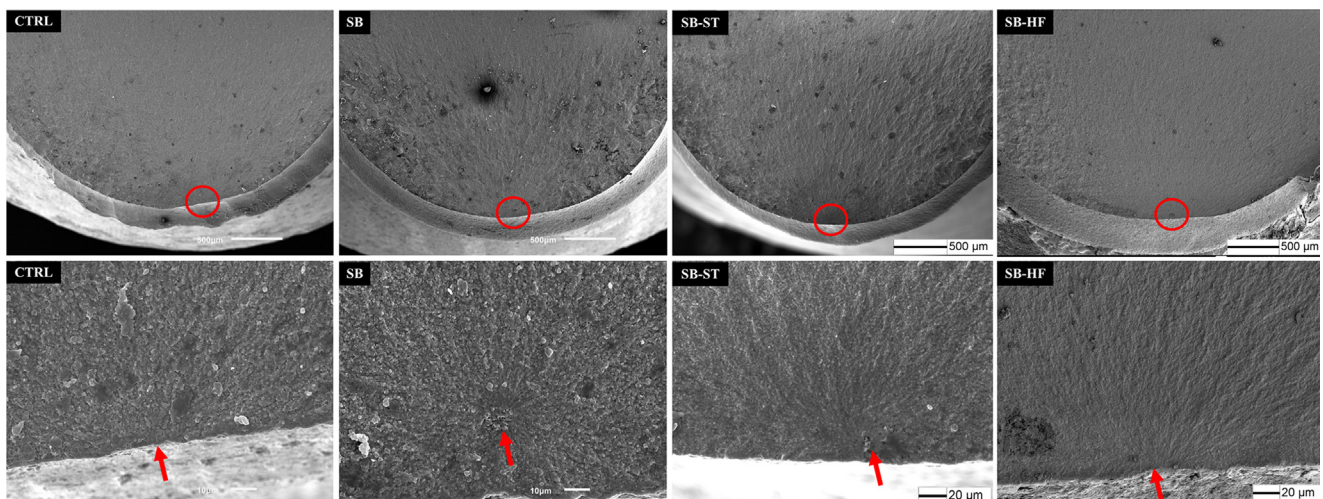


Fig. 6. SEM photographs of the fractured surfaces after the cyclic fatigue test (red circle and arrow show the crack origin). (For interpretation of the references to color in this figure legend, the reader is referred to the web version of this article.)

titanium implant/abutment systems (Rosentritt et al., 2014). The static and fatigue strengths of Y-TZP were improved owing to transformation toughening, which was not observed with titanium. Moreover, the favorable mechanical properties of Y-TZP blocks and the used manufacturing method may also be the possible reasons for the high fatigue strength achieved in this study.

In previous clinical studies evaluating biting and chewing forces, Fontijn-Tekamp et al. (2000) reported the maximum bite forces in the posterior dentition ranging from 250 N to 400 N, and in the anterior dentition ranging from 140 N to 170 N. Sathyanarayana et al. (2012) reported the mean maximum voluntary bite force in the molar and first premolar regions to be  $601.83 \text{ N} \pm 60.80$  and  $392 \text{ N} \pm 31.43$ , respectively, in adults with normal occlusion. It should be noted that the implants were angled by  $30^\circ \pm 2^\circ$  to the loading direction of the testing machine instead of axial loading to simulate functional load under the worst possible in vivo conditions. This situation introduced both vertical and horizontal loads. The fatigue strength of CAD/CAM zirconia implant exceeded the maximum bite force of both the anterior and posterior dentition reported in the literature. Even after a simulated intraoral loading period of 25 years, the mean fracture strength values of zirconia implants were  $1059.3 \pm 165.1 \text{ N}$ . These results indicate that such an implant is capable of withstanding clinical occlusal loading for more than 25 years.

Nevertheless, extreme caution should always be taken in drawing conclusions for clinical situations based on laboratory results. Multiple variables that are normally present in vivo and affecting fatigue strength are generally excluded in a controlled laboratory research environment.

#### 4.5. Slow crack growth and the ratio of fatigue strength to fracture strength

Fatigue failure of ceramic materials, including zirconia, is controlled by slow crack growth (SCG) of pre-existing cracks or flaws (Ritter and Humenik, 1979). Fracture of ceramics occurs when the stress intensity factor ( $K_I$ ) at the crack tip reaches a critical level ( $K_{IC}$ ). Under cyclic loading, the presence of stresses and water molecules at the crack tip can reduce the surface energy and cause crack propagation. Then the cracks grow continuously and slowly under loads lower than the critical value, with a stress intensity factor lower than  $K_{IC}$ , until reaching the critical size for failure, leading to catastrophic failure of the implants (Amaral et al., 2016; Wang et al., 2008).

Fortunately, the presence of a threshold stress intensity factor  $K_{I0}$ , below which no crack propagation occurs, has been claimed in previous literatures (Sanon et al., 2015; Chevalier et al., 2000). This can explain the fact that zirconia implants in this study could survive up to  $5 \times 10^6$  loading cycles under loads lower than fatigue limit. The ratio of fatigue limit to fracture strength may be appropriately equivalent to the ratio of  $K_{I0}$  to  $K_{IC}$  of 3Y-TZP, which has been reported to be roughly 0.5 (Sanon et al., 2015). Consistent with this, the ratio of fatigue limit to fracture strength of zirconia implants in this study ranges from 0.57 to 0.64.

#### 4.6. Limitations

One limitation of this study is that the testing was conducted at room temperature, different from the oral environment. The oral environment has many elements that favor SCG in zirconia, such as water and pH variations from saliva, masticatory stresses, and temperature (Morena et al., 1986; Pinto et al., 2008). It is not well known how the combination of stresses, temperature, humidity, and saliva in the oral environment affects the phase transformation and fatigue strength of zirconia implants.

The metastability of zirconia leads to phase transformation in contact with water with time. This phenomenon is referred as low-temperature degradation (LTD) or aging (Sanon et al., 2013). Aging is a progressive  $t \rightarrow m$  transformation at the surface triggered by water molecules, often resulting in surface roughening and microcracking and

thus potentially influencing the mechanical properties. Sanon (Sanon et al., 2013) reported a higher fatigue performance of Y-TZP implants with a porous surface after aging at  $134^\circ \text{C}$  and 0.2 MPa for 20 h. However, Flinn (Flinn et al., 2012) found that accelerated aging at  $134^\circ \text{C}$  and 0.2 MPa for 200 h caused a significant reduction in the mean flexural strength of three brands of zirconia due to LTD. Further study is needed to determine the effect of LTD on the fatigue resistance of CAD/CAM zirconia implants with different surface treatments.

Moreover, the fracture and fatigue strengths amongst the four groups showed similar variation tendencies, except for the static strength of the SB and SB-ST groups. The possible reason for these inconsistencies is the presence of non-uniform flaws and microcracks on the zirconia implant surface due to the CAM process (Fig. 3). If the flaws and microcracks are located at the tensile stress side surface of the zirconia implants, they may have a negative impact on the static strength, particularly because of the fewer number of specimens used in the static testing.

Traditionally, prefabricated standardized implants were widely used in clinical practices. However, the clinical condition varies for individual patients. Based on the findings reported in this study, it is feasible and promising to use CAD/CAM technology to design and fabricate customized zirconia implants according to individual patient's hard and soft tissue characteristics assessed using cone beam CT scan. This customized zirconia implant is expected to simplify the procedures of implant treatment, minimize trauma to the hard and soft tissues, and improve the functional and esthetic outcomes of implant prostheses (Pirker and Kochev, 2011; Figliuzzi et al., 2012). This novel approach can be an alternative method for immediate or delayed implantation and will possibly raise the bar for dental implantology to a higher level of individualization.

## 5. Conclusion

Within the limitations of this study, it can be concluded that a CAD/CAM zirconia implant has a favorable fracture and fatigue resistance. Compared to sintering, sandblasting or sandblasting and experimental hot acid solution etching achieved moderately rough surfaces ( $R_a$ , 1–2  $\mu\text{m}$ ) and resulted in a higher fracture and fatigue resistance of CAD/CAM zirconia implants. However, sandblasting and hydrofluoric acid etching resulted in the roughest surfaces without increasing fracture and fatigue resistance. The results of this study indicate that the CAD/CAM zirconia implants with roughening surfaces may have sufficient fatigue strength to satisfy the routine clinical demand.

## Acknowledgements

This work was supported by the National Natural Science Foundation of China [grant number 81671026].

## Declarations of interest

None.

## References

- Amaral, M., Cesar, P.F., Bottino, M.A., Lohbauer, U., Valandro, L.F., 2016. Fatigue behavior of y-tzp ceramic after surface treatments. *J. Mech. Behav. Biomed. Mater.* 57, 149–156. <http://dx.doi.org/10.1016/j.jmbm.2015.11.042>.
- Andrioteelli, M., Wenz, H.J., Kohal, R.J., 2009. Are ceramic implants a viable alternative to titanium implants? A systematic literature review. *Clin. Oral Implants Res.* 20 (Suppl. 4), S32–S47. <http://dx.doi.org/10.1111/j.1600-0501.2009.01785.x>.
- Assenza, B., Tripodi, D., Scarano, A., Perrotti, V., Piattelli, A., Iezzi, G., D'Ercole, S., 2012. Bacterial leakage in implants with different implant-abutment connections: an in vitro study. *J. Periodontol.* 83, 491–497. <http://dx.doi.org/10.1902/jop.2011.110320>.
- Brull, F., van Winkelhoff, A.J., Cune, M.S., 2014. Zirconia dental implants: a clinical, radiographic, and microbiologic evaluation up to 3 years. *Int. J. Oral Maxillofac. Implants* 29, 914–920.
- Casucci, A., Osorio, E., Osorio, R., Monticelli, F., Toledano, M., Mazzitelli, C., Ferrari, M.,

2009. Influence of different surface treatments on surface zirconia frameworks. *J. Dent.* 37, 891–897. <http://dx.doi.org/10.1016/j.jdent.2009.06.013>.
- Chevalier, J., Aza, A., Fantozzi, G., Schehl, M., Torrecillas, R., 2000. Extending the life-time of ceramic orthopaedic implants. *Adv. Mater.* 12, 1619–1621.
- Chintapalli, R.K., Mestra, R.A., Garcia, M.F., Anglada, M., 2014. Effect of sandblasting and residual stress on strength of zirconia for restorative dentistry applications. *J. Mech. Behav. Biomed. Mater.* 29, 126–137. <http://dx.doi.org/10.1016/j.jmbbm.2013.09.004>.
- Denry, I., Kelly, J.R., 2008. State of the art of zirconia for dental applications. *Dent. Mater.* 24, 299–307. <http://dx.doi.org/10.1016/j.dental.2007.05.007>.
- Egilmaz, F., Ergun, G., Cekiç-Nagas, I., Vallittu, P.K., Lassila, L.V., 2014. Factors affecting the mechanical behavior of y-tzp. *J. Mech. Behav. Biomed. Mater.* 37, 78–87. <http://dx.doi.org/10.1016/j.jmbbm.2014.05.013>.
- Figliuzzi, M., Mangano, F., Mangano, C., 2012. A novel root analogue dental implant using ct scan and cad/cam: selective laser melting technology. *Int. J. Oral Maxillofac. Surg.* 41, 858–862. <http://dx.doi.org/10.1016/j.ijom.2012.01.014>.
- Flamant, Q., Anglada, M., 2016. Hydrofluoric acid etching of dental zirconia. Part 2: effect on flexural strength and ageing behavior. *J. Eur. Ceram. Soc.* 36, 135–145. <http://dx.doi.org/10.1016/j.jeurceramsoc.2015.09.022>.
- Flinn, B.D., DeGroot, D.A., Mancl, L.A., Raigrodski, A.J., 2012. Accelerated aging characteristics of three yttria-stabilized tetragonal zirconia polycrystalline dental materials. *J. Prosthet. Dent.* 108, 223–230. [http://dx.doi.org/10.1016/S0022-3913\(12\)60166-8](http://dx.doi.org/10.1016/S0022-3913(12)60166-8).
- Fontijn-Tekamp, F.A., Slagter, A.P., Van Der Bilt, A., Van T, H.M., Witter, D.J., Kalk, W., Jansen, J.A., 2000. Biting and chewing in overdentures, full dentures, and natural dentitions. *J. Dent. Res.* 79, 1519–1524.
- Gahlert, M., Gudehus, T., Eichhorn, S., Steinhauser, E., Kniha, H., Erhardt, W., 2007. Biomechanical and histomorphometric comparison between zirconia implants with varying surface textures and a titanium implant in the maxilla of miniature pigs. *Clin. Oral Implants Res.* 18, 662–668. <http://dx.doi.org/10.1111/j.1600-0501.2007.01401.x>.
- Gahlert, M., Bertscher, D., Grunert, I., Kniha, H., Steinhauser, E., 2012. Failure analysis of fractured dental zirconia implants. *Clin. Oral Implants Res.* 3, 287–293. <http://dx.doi.org/10.1111/j.1600-0501.2011.02206.x>.
- García, F.R., de Oliveira, A.F., Dos, S.N.R.J., Rambaldi, E., Baldissara, P., 2013. Effect of particle size on the flexural strength and phase transformation of an airborne-particle abraded yttria-stabilized tetragonal zirconia polycrystal ceramic. *J. Prosthet. Dent.* 110, 510–514. <http://dx.doi.org/10.1016/j.prosdent.2013.07.007>.
- Gil, F.J., Espinar, E., Llamas, J.M., Sevilla, P., 2014. Fatigue life of bioactive titanium dental implants treated by means of grit-blasting and thermo-chemical treatment. *Clin. Implant Dent. Relat. Res.* 16, 273–281. <http://dx.doi.org/10.1111/j.1708-8208.2012.00468.x>.
- Guazzato, M., Albakry, M., Ringer, S.P., Swain, M.V., 2004. Strength, fracture toughness and microstructure of a selection of all-ceramic materials. Part ii. Zirconia-based dental ceramics. *Dent. Mater.* 20, 449–456. <http://dx.doi.org/10.1016/j.dental.2003.05.002>.
- Huang, H.M., Tsai, C.M., Chang, C.C., Lin, C.T., Lee, S.Y., 2005. Evaluation of loading conditions on fatigue-failed implants by fracture surface analysis. *Int. J. Oral Maxillofac. Implants* 20, 854–859.
- Iijima, T., Homma, S., Sekine, H., Sasaki, H., Yajima, Y., Yoshinari, M., 2013. Influence of surface treatment of yttria-stabilized tetragonal zirconia polycrystal with hot isostatic pressing on cyclic fatigue strength. *Dent. Mater. J.* 32, 274–280.
- ISO/DIS 14801, 2014. Dentistry-implants-dynamic fatigue test for endosseous dental implants. *Int. Organ. Stand.*
- Karakoca, S., Yilmaz, H., 2009. Influence of surface treatments on surface roughness, phase transformation, and biaxial flexural strength of y-tzp ceramics. *J. Biomed. Mater. Res. B Appl. Biomater.* 91, 930–937. <http://dx.doi.org/10.1002/jbm.b.31477>.
- Katagiri, G., Ishida, H., Ishitani, A., Masaki, T., 1988. Direct determination by a raman microprobe of the transformation zone size in y2o3 containing tetragonal zro2 polycrystals. *Adv. Ceram.* 537–544.
- Kim, J.W., Covell, N.S., Guess, P.C., Rewok, E.D., Zhang, Y., 2010. Concerns of hydrothermal degradation in cad/cam zirconia. *J. Dent. Res.* 89, 91–95. <http://dx.doi.org/10.1177/0022034509354193>.
- Kohal, R.J., Wolkewitz, M., Tsakona, A., 2011. The effects of cyclic loading and preparation on the fracture strength of zirconium-dioxide implants: an in vitro investigation. *Clin. Oral Implants Res.* 22, 808–814. <http://dx.doi.org/10.1111/j.1600-0501.2010.02067.x>.
- Kosma, T., Oblak, E., Marion, L., 2008. The effects of dental grinding and sandblasting on ageing and fatigue behavior of dental zirconia (y-tzp) ceramics. *J. Eur. Ceram. Soc.* 28, 1085–1090. <http://dx.doi.org/10.1016/j.jeurceramsoc.2007.09.013>.
- Kosmac, T., Oblak, C., Jevnikar, P., Funduk, N., Marion, L., 2000. Strength and reliability of surface treated y-tzp dental ceramics. *J. Biomed. Mater. Res.* 53, 304–313.
- Koyama, T., Sato, T., Yoshinari, M., 2012. Cyclic fatigue resistance of yttria-stabilized tetragonal zirconia polycrystals with hot isostatic press processing. *Dent. Mater. J.* 31, 1103–1110.
- Lee, C.K., Karl, M., Kelly, J.R., 2009. Evaluation of test protocol variables for dental implant fatigue research. *Dent. Mater.* 25, 1419–1425. <http://dx.doi.org/10.1016/j.dental.2009.07.003>.
- Luthardt, R.G., Holzhuber, M.S., Rudolph, H., Herold, V., Walter, M.H., 2004. Cad/cam-machining effects on y-tzp zirconia. *Dent. Mater.* 20, 655–662. <http://dx.doi.org/10.1016/j.dental.2003.08.007>.
- Morena, R., Beaudreau, G.M., Lockwood, P.E., Evans, A.L., Fairhurst, C.W., 1986. Fatigue of dental ceramics in a simulated oral environment. *J. Dent. Res.* 65, 993–997. <http://dx.doi.org/10.1177/00220345860650071901>.
- Morgan, M.J., James, D.F., Pilliar, R.M., 1993. Fractures of the fixture component of an osseointegrated implant. *Int. J. Oral Maxillofac. Implants* 8, 409–414.
- Nemli, S.K., Yilmaz, H., Aydin, C., Bal, B.T., Tiras, T., 2012. Effect of fatigue on fracture toughness and phase transformation of y-tzp ceramics by x-ray diffraction and raman spectroscopy. *J. Biomed. Mater. Res. B Appl. Biomater.* 100, 416–424. <http://dx.doi.org/10.1002/jbm.b.31964>.
- Oliva, J., Oliva, X., Oliva, J.D., 2007. One-year follow-up of first consecutive 100 zirconia dental implants in humans: a comparison of 2 different rough surfaces. *Int. J. Oral Maxillofac. Implants* 22, 430–435.
- Oliva, J., Oliva, X., Oliva, J.D., 2010. Five-year success rate of 831 consecutively placed zirconia dental implants in humans: a comparison of three different rough surfaces. *Int. J. Oral Maxillofac. Implants* 25, 336–344.
- Ozcan, M., Melo, R.M., Souza, R.O., Machado, J.P., Felipe, V.L., Bottino, M.A., 2013. Effect of air-particle abrasion protocols on the biaxial flexural strength, surface characteristics and phase transformation of zirconia after cyclic loading. *J. Mech. Behav. Biomed. Mater.* 20, 19–28. <http://dx.doi.org/10.1016/j.jmbbm.2013.01.005>.
- Ozkurt, Z., Kazazoglu, E., 2011. Zirconia dental implants: a literature review. *J. Oral Implantol.* 37, 367–376. <http://dx.doi.org/10.1563/AAID-JOI-D-09-00079>.
- Piconi, C., Maccauro, G., 1999. Zirconia as a ceramic biomaterial. *Biomaterials* 20, 1–25.
- Pinto, M.M., Cesar, P.F., Rosa, V., Yoshimura, H.N., 2008. Influence of ph on slow crack growth of dental porcelains. *Dent. Mater.* 24, 814–823. <http://dx.doi.org/10.1016/j.dental.2007.10.001>.
- Pirker, W., Kocher, A., 2011. Root analog zirconia implants: true anatomical design for molar replacement—a case report. *Int. J. Periodontics Restor. Dent.* 31, 663–668.
- Pittayachawan, P., McDonald, A., Young, A., Knowles, J.C., 2009. Flexural strength, fatigue life, and stress-induced phase transformation study of y-tzp dental ceramic. *J. Biomed. Mater. Res. B Appl. Biomater.* 88, 366–377. <http://dx.doi.org/10.1002/jbm.b.31064>.
- Porter, D.L., Heuer, A.H., 1977. Mechanisms of toughening partially stabilized zirconia (psz). *J. Am. Ceram. Soc.* 183–184.
- Raigrodski, A.J., 2004. Contemporary materials and technologies for all-ceramic fixed partial dentures: a review of the literature. *J. Prosthet. Dent.* 92, 557–562. <http://dx.doi.org/10.1016/S0022391304006158>.
- Rita Deprich, C.N., 2012. Current findings regarding zirconia implants. *Clin. Implant Dent. Res.* 1–12.
- Ritter, J., Humenik, J., 1979. Static and dynamic fatigue of polycrystalline alumina. *J. Membr. Sci.* 14, 1573–4803.
- Roehling, S., Woelfler, H., Hicklin, S., Kniha, H., Gahlert, M., 2015. A retrospective clinical study with regard to survival and success rates of zirconia implants up to and after 7 years of loading. *Clin. Implant Dent. Relat. Res.* <http://dx.doi.org/10.1111/cid.12323>.
- Rosentritt, M., Hagemann, A., Hahnel, S., Behr, M., Preis, V., 2014. In vitro performance of zirconia and titanium implant/abutment systems for anterior application. *J. Dent.* 42, 1019–1026. <http://dx.doi.org/10.1016/j.jdent.2014.03.010>.
- Sanon, C., Chevalier, J., Douillard, T., Kohal, R.J., Coelho, P.G., Hjerpe, J., Silva, N.R., 2013. Low temperature degradation and reliability of one-piece ceramic oral implants with a porous surface. *Dent. Mater.* 29, 389–397. <http://dx.doi.org/10.1016/j.dental.2013.01.007>.
- Sanon, C., Chevalier, J., Douillard, T., Cattani-Lorente, M., Scherrer, S.S., Gremillard, L., 2015. A new testing protocol for zirconia dental implants. *Dent. Mater.* 31, 15–25. <http://dx.doi.org/10.1016/j.dental.2014.09.002>.
- Sathyanarayana, H.P., Premkumar, S., Manjula, W.S., 2012. Assessment of maximum voluntary bite force in adults with normal occlusion and different types of mal-occlusions. *J. Contemp. Dent. Pract.* 13, 534–538.
- Scarano, A., Piattelli, A., Polimeni, A., Di Iorio, D., Carinci, F., 2010. Bacterial adhesion on commercially pure titanium and anatase-coated titanium healing screws: an in vivo human study. *J. Periodontol.* 81, 1466–1471. <http://dx.doi.org/10.1902/jop.2010.100061>.
- Sennerby, L., Dasmah, A., Larsson, B., Iverhed, M., 2005. Bone tissue responses to surface-modified zirconia implants: a histomorphometric and removal torque study in the rabbit. *Clin. Implant Dent. Relat. Res.* 7 (Suppl. 1), S13–S20.
- Sevilla, P., Sandino, C., Arciniegas, M., 2010. Evaluating mechanical properties and degradation of ytzp dental implants. *Mater. Sci. Eng. C* 14–19.
- Shemtov-Yona, K., Rittel, D., Levin, L., Machtei, E.E., 2014. Effect of dental implant diameter on fatigue performance. Part i: mechanical behavior. *Clin. Implant Dent. Relat. Res.* 16, 172–177. <http://dx.doi.org/10.1111/j.1708-8208.2012.00477.x>.
- Silva, N.R., Coelho, P.G., Fernandes, C.A., Navarro, J.M., Dias, R.A., Thompson, V.P., 2009. Reliability of one-piece ceramic implant. *J. Biomed. Mater. Res. B Appl. Biomater.* 88, 419–426. <http://dx.doi.org/10.1002/jbm.b.31113>.
- Tete, S., Mastrangelo, F., Bianchi, A., Zizzari, V., Scarano, A., 2009. Collagen fiber orientation around machined titanium and zirconia dental implant necks: an animal study. *Int. J. Oral Maxillofac. Implants* 24, 52–58.
- Wang, H., Aboushelbi, M.N., Feilzer, A.J., 2008. Strength influencing variables on cad/cam zirconia frameworks. *Dent. Mater.* 24, 633–638. <http://dx.doi.org/10.1016/j.dental.2007.06.030>.
- Xie, H., Shen, S., Qian, M., Zhang, F., Chen, C., Tay, F.R., 2015. Effects of acid treatment on dental zirconia: an in vitro study. *PLoS One* 10, e136263. <http://dx.doi.org/10.1371/journal.pone.0136263>.